

Deformation Potentials of Lead Telluride*†

LUIZ G. FERREIRA‡

*Materials Theory Group, Department of Electrical Engineering,
Massachusetts Institute of Technology, Cambridge, Massachusetts*

(Received 3 June 1964; revised manuscript received 21 September 1964)

A computer calculation of the important deformation potentials of PbTe was made. The calculation was based on an extension of the augmented-plane-wave method. Group theory was extensively used in connection with the reduction of the cubic group of this material by a uniaxial strain. The calculated pressure coefficient of the energy gap is in excellent agreement with experiment. This fact confirms that the highest valence band is an L_1^+ state at the edge of the Brillouin zone, along the (111) direction. The calculated coefficients for shear strain do not agree with the numbers derived from experimental work. Here, it is felt that incomplete models were assumed in the analysis of the experiments. In particular, it is suggested that the intravalley one-phonon acoustical model for scattering of carriers is inadequate for lead telluride.

I. INTRODUCTION

THE present article is a report on a computer calculation of the properties of lead telluride under a general strain. The starting point of the calculation is the set of eigenvalues and wave functions, obtained during the band structure calculation for this material.¹ The method for calculation of the deformation potentials is an expansion of the augmented-plane-wave (APW) method; the crystal potential for the deformed lattice is defined analogously. Then, with the definition of the deformed potential, it is possible to find an expression for the strain Hamiltonian.

In Sec. II, the *strain Hamiltonian* of Pikus and Bir² is presented, its symmetry is discussed, and the effects of strain on the important electronic states are derived by means of group theory. In Sec. III, the numerical values of the important matrix elements of the strain Hamiltonian are presented, the linear relations among these matrix elements are discussed, and a brief introduction to the method of calculation is made. In Sec. IV, the effects of spin-orbit interaction, on the strain formalism, are discussed. It is then shown that, because the levels become nondegenerate,³ the effects of strain on each level, at the point L of the Brillouin zone, can be described by $\delta E = D_{ij}\epsilon_{ij}$. Here, δE is the change in the energy due to the strain tensor ϵ_{ij} , and D_{ij} is the *deformation potential* tensor. For reasons of symmetry, the deformation potential tensor, for the states at the point L , can be written as $D_{ij} = D_d\delta_{ij} + D_u u_i u_j$, where $(u_1 u_2 u_3)$ is the unit vector along (111). At the center

of the zone, the important Γ_8^- state is treated by means of the formalism of Kleiner and Roth.⁴ The numerical results are then compared with some results from experimental work, and two important conclusions are drawn:

1. The highest state in the valence band is a L_1^+ state, and not a L_3^+ as it was thought formerly.⁵
2. The scattering of current carrying electrons and holes is *not* the intravalley one-phonon acoustical process (deformation potential model).

II. STRAIN HAMILTONIAN AND SYMMETRY CONSIDERATIONS

As shown by Pikus and Bir,² if in Schrödinger's equation for a strained crystal

$$[-\nabla^2 + V^S(\mathbf{r})]\psi_k^S(\mathbf{r}) = E\psi_k^S(\mathbf{r}),$$

we substitute the values $(\delta_{ij} + \epsilon_{ij})x_j$ for the variables x_i ($i=1, 2, 3$), we obtain

$$[-\nabla^2 + V_0(\mathbf{r}) + \epsilon_{ij}S_{ij}(\mathbf{r})]\psi_k(\mathbf{r}) = E\psi_k(\mathbf{r}). \quad (1)$$

In Eq. (1), the symbol $V_0(\mathbf{r})$ stands for the self-consistent potential of the unstrained crystal and $S_{ij}(\mathbf{r})$ is the *strain Hamiltonian*. $V^S(\mathbf{r})$ is the self-consistent potential for the strained lattice, and we have neglected terms that are second-order in the strain components. The explicit expression for the strain Hamiltonian is given by

$$S_{ij}(\mathbf{r}) = 2(\partial/\partial x_i)(\partial/\partial x_j) + V_{ij}(\mathbf{r}), \quad (2)$$

where $V_{ij}(\mathbf{r})$ is defined by

$$V_{ij}(\mathbf{r}) = \lim_{\epsilon_{ij} \rightarrow 0} \frac{V^S(x_i - \epsilon_{ij}x_j) - V_0(x_i)}{\epsilon_{ij}}.$$

It can be shown, by a simple argument, that the strain Hamiltonian transforms as follows: Let R be an

* This work was supported by the Office of Naval Research [Contract No. Nonr-1841(51)] and the Army Research Office (Durham-Contract No. DA-31-124-ARO(D)-92).

† This report is based on a thesis submitted to the Department of Electrical Engineering, MIT, in partial fulfillment of the requirements for the degree of Doctor of Philosophy.

‡ Present address: Instituto Tecnológico de Aeronautica, São José dos Campos, S.P., Brazil.

¹ J. B. Conklin, Jr., Electrical Engineering Department, MIT, Doctoral thesis 1964 (unpublished).

² G. E. Pikus and G. L. Bir, *Fiz. Tverd. Tela* **1**, 1642 (1959) [English transl.: *Soviet Phys.—Solid State* **1**, 1502 (1959)].

³ In fact, there is the time-reversal degeneracy, which simply doubles the number of states in each band. This degeneracy, for the rock salt structure of lead telluride, is never destroyed by a strain deformation.

⁴ W. H. Kleiner and L. M. Roth, *Phys. Rev. Letters* **2**, 334 (1959).

⁵ L. E. Johnson, J. B. Conklin, Jr., and G. W. Pratt, Jr., *Phys. Rev. Letters* **11**, 538 (1963).

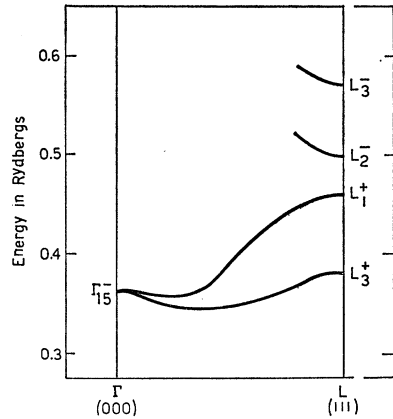


FIG. 1. Some important single-group states in PbTe (schematic).

operation of the point group, and let a_{ij} be the matrix that rotates a vector \mathbf{v} by R , or

$$R\mathbf{v} = a_{ij}v_j.$$

Then, there follows the relation

$$RS_{ij}(\mathbf{r})R^{-1} = a_{ni}S_{nm}(\mathbf{r})a_{mj} = S_{ij}(R^{-1}\mathbf{r}). \quad (3)$$

If we now apply the operator R to Eq. (1), there results

$$[-\nabla^2 + V_0(\mathbf{r}) + a_{ni}\epsilon_{ij}a_{mj}S_{nm}(\mathbf{r})]\psi_{Rk}(\mathbf{r}) = E\psi_{Rk}(\mathbf{r}), \quad (4)$$

which clearly shows that the eigenvalue E remains constant, if both the strain tensor ϵ_{ij} and the wave vector \mathbf{k} are rotated by the same operation.

In order to fully describe the effects of strain on a given energy level, we have to deal with the six independent components of the tensor ϵ_{ij} . This general strain tensor can be described in a better way: Consider seven uniaxial strains along the crystallographic directions (100), (010), (001), (111), ($\bar{1}\bar{1}\bar{1}$), ($1\bar{1}\bar{1}$), and ($\bar{1}\bar{1}1$) in the cubic system of PbTe. By a uniaxial strain ϵ along the direction given by the unit vector \mathbf{u} we mean the tensor $\epsilon\mathbf{u}\mathbf{u}$. It can be shown that the components ϵ_{ij} of the general strain tensor can be expanded, in terms of uniaxial strains along the principal directions, according to Table I.

The most important states at Γ (center of the Brillouin zone) and at L (center of the hexagonal face perpendicular to the (111) direction) are plotted in Fig. 1. This is a schematic drawing based on the band calculation.¹ The actual position of the states was slightly corrected to account for some experimental facts. The results on which Fig. 1 is based include the mass-velocity and the $\mathbf{E}\cdot\mathbf{p}$ corrections, but exclude the spin-orbit interaction. It has been proven that Γ and L are the most important points, in the Brillouin zone, for the conduction processes.^{1,6,7} The labeling of states

⁶ K. F. Cuff, M. R. Ellett, and C. D. Kuglin, *Proceedings of the International Conference on the Physics of Semiconductors, Exeter, July 1962* (The Institute of Physics and the Physical Society, London, 1962), p. 316.

⁷ P. J. Stiles, E. Burstein, and D. N. Langenberg, *Proceedings of the International Conference on the Physics of Semiconductors Exeter, July 1962* (The Institute of Physics and the Physical Society, London, 1962), p. 577.

TABLE I. Coefficients for the linear expansion of the strain components ϵ_{ij} in terms of the uniaxial strains along the important cubic directions.^a

	ϵ_{100}	ϵ_{010}	ϵ_{001}	ϵ_{111}	$\epsilon_{1\bar{1}\bar{1}}$	$\epsilon_{\bar{1}\bar{1}1}$	$\epsilon_{\bar{1}\bar{1}1}$
ϵ_{11}	1	0	0	$\frac{1}{3}$	$\frac{1}{3}$	$\frac{1}{3}$	$\frac{1}{3}$
ϵ_{22}	0	1	0	$\frac{1}{3}$	$\frac{1}{3}$	$\frac{1}{3}$	$\frac{1}{3}$
ϵ_{33}	0	0	1	$\frac{1}{3}$	$\frac{1}{3}$	$\frac{1}{3}$	$\frac{1}{3}$
ϵ_{12}	0	0	0	$\frac{1}{3}$	$\frac{1}{3}$	$-\frac{1}{3}$	$-\frac{1}{3}$
ϵ_{13}	0	0	0	$\frac{1}{3}$	$-\frac{1}{3}$	$-\frac{1}{3}$	$-\frac{1}{3}$
ϵ_{23}	0	0	0	$\frac{1}{3}$	$-\frac{1}{3}$	$-\frac{1}{3}$	$\frac{1}{3}$

^a A uniaxial strain ϵ along a direction \mathbf{u} is here defined by $\epsilon\mathbf{u}\mathbf{u}$. The symbols $\epsilon_{100}, \dots, \epsilon_{111}$ mean uniaxial strains along the (100), \dots , ($\bar{1}\bar{1}\bar{1}$) cubic directions, respectively.

according to the names of their irreducible representations was made for the center of symmetry located at the lead site. The corresponding names of the representations, when a tellurium site is chosen as the center of symmetry, are presented in Table II. In that table, we also exhibit the way the partners of the irreducible representations transform, under the rotation of the group.

From Eq. (4) we know that, for the point Γ , the strains (100), (010), and (001), and ($1\bar{1}\bar{1}$), ($\bar{1}\bar{1}1$), ($\bar{1}\bar{1}\bar{1}$),

TABLE II. Correspondence between representations for center of symmetry at lead and tellurium sites.

Lead site Transform as the functions of the coordinates ^a	Repre- sentation name	Repre- sentation name	Tellurium site Transform as the functions of the coordinates ^a
(x,y)	L_3^-	L_3^+	(zx,zy)
(z)	L_2^-	L_1^+	(1)
(1)	L_1^+	L_2^-	(z)
(zx,zy)	L_3^+	L_3^-	(x,y)
(x,y,z)	Γ_{15}^-	Γ_{15}^-	(x,y,z)

^a The x , y , and z axes are oriented along the ($1\bar{1}0$), ($11\bar{2}$), and (111) directions, respectively.

and (111) are equivalent; while for the point L along the (111) direction, the uniaxial strains (100), (010), and (001), and ($\bar{1}\bar{1}\bar{1}$), ($1\bar{1}\bar{1}$), and ($1\bar{1}\bar{1}$) lead to equivalent eigenvalues. Therefore, we can describe the effects on Γ of any strain tensor in terms of the effects of the uniaxial strains along (001) and (111) only. For the point L , the uniaxial strains along (001), (111), and ($1\bar{1}\bar{1}$) are sufficient to determine the whole behavior of the bands.

TABLE III. Group of the wave vector at $\Gamma(000)$ (point group of the crystal).

	E	$3C_2$	$6C_4$	$8C_3$	$6C_2$
Γ_1^C	1	1	1	1	1
Γ^C	1	1	-1	1	-1
Γ_{12}^C	2	2	0	-1	0
Γ_{15}^C	3	-1	1	0	-1
Γ_{25}^C	3	-1	-1	0	1

^a Superscript C stands for the cubic symmetry.

TABLE IV. Group at $\Gamma(000)$ when reduced by a uniaxial strain along (001). The following relation holds: $\Gamma_{15}^{C-} = \Gamma_2^{T-} + \Gamma_5^{T-}$.^a

	E	C_4^2	$2C_4$	$2C_2$	$2C_2'$
Γ_1^{Tb}	1	1	1	1	1
Γ_2^{T-}	1	1	1	-1	-1
Γ_3^{T-}	1	1	-1	1	-1
Γ_4^{T-}	1	1	-1	-1	1
Γ_5^{T-}	2	-2	0	0	0

^a See Table III.
^b Superscript T stands for the tetragonal distortion.

We can see the effects of the uniaxial strain deformations, mentioned in the preceding paragraph, by means of group theory. According to Eq. (4), the group that leaves the total Hamiltonian invariant is the subgroup of the point group that transforms the strain tensor ϵ_{ij} into itself. Therefore, a uniaxial strain deformation preserves only the following operations: inversion, the rotations about the axis of strain, the dyad axes perpendicular to the strain direction, and the operations derived therefrom by product combinations. The group of the wave vector at Γ , or better, its character table, is given in Table III. A uniaxial strain along (001) creates a *tetragonal* distortion, so that the group at Γ

TABLE V. Group at $\Gamma(000)$ when reduced by a uniaxial strain along (111). The following relation holds: $\Gamma_{15}^{C-} = \Gamma_2^{R-} + \Gamma_3^{R-}$.^a

	E	$2C_3$	$3C_2$
Γ_1^{Rb}	1	1	1
Γ_2^{R-}	1	1	-1
Γ_3^{R-}	2	-1	0

^a See Table III.
^b Superscript R stands for the rhombohedral distortion.

becomes reduced to that of Table IV. In that table, it is also shown how the irreducible representation Γ_{15}^{C-} , of the cubic group, splits under the tetragonal distortion. A uniaxial strain along (111) creates a *rhombohedral* distortion, and reduces the cubic group to that of Table V. For the point L along (111), the group of the wave vector is given by Table VI. A uniaxial strain along (111) does not reduce the group of Table VI, but a uniaxial strain along (11 $\bar{1}$) reduces it to the group of Table VII. Finally, a uniaxial strain along (001) reduces the group of the wave vector at L to that of Table VIII. It is worth mentioning that in Tables III–VIII, the improper rotations have been

TABLE VI. Group of the wave vector at $L(111)$. (A uniaxial strain along (111) does not reduce this group.)

	E	$2C_3$	$3C_2$
L_1^{Ca}	1	1	1
L_2^C	1	1	-1
L_3^C	2	-1	0

^a Superscript C stands for the cubic symmetry.

deliberately omitted, and each of the irreducible representations may be of even or odd parity.

III. RESULTS AND METHOD OF COMPUTATION

The results were derived by means of the APW method. In the APW method, the space occupied by the crystal is filled with nonoverlapping spheres, around the atoms, inside which spherically symmetrical potentials are assumed. Outside the spheres the potential is approximated by a constant. The best value for this constant is somewhat uncertain, but the following rule has been shown to be a good one: The spheres are made

TABLE VII. Group at $L(111)$ when reduced by a uniaxial strain along (11 $\bar{1}$). The following relations hold: $L_1^{C+} = L_1^{R+}$; $L_2^{C-} = L_2^{R-}$; $L_3^{C+} = L_1^{R+} + L_2^{R+}$; $L_3^{C-} = L_1^{R-} + L_2^{R-}$.^a

	E	C_2
L_1^{Rb}	1	1
L_2^{R-}	1	-1

^a See Table VI.
^b Superscript R stands for the rhombohedral distortion.

to touch; their radii are chosen so that the inside potentials, for the different atomic species, become equal at the sphere surfaces; the constant outside the spheres is made equal to the value of the inside potentials at the sphere surfaces. This rule leads to a continuous crystal potential, and has been yielding results that are comparable with experiment.

For a consistent definition of the strain Hamiltonian, we must have a rule for the construction of the crystal potential in the strained lattice. Because of the strain, the touching spheres of the normal lattice become touching ellipsoids. Inside the ellipsoids, the same

TABLE VIII. Group at $L(111)$ when reduced by a uniaxial strain along (001). The following relations hold: $L_1^{C+} = L_1^{T+}$; $L_2^{C-} = L_2^{T-}$; $L_3^{C+} = L_1^{T+} + L_2^{T+}$; $L_3^{C-} = L_1^{T-} + L_2^{T-}$.^a

	E	C_2
L_1^{Tb}	1	1
L_2^{T-}	1	-1

^a See Table VI.
^b Superscript T stands for the tetragonal distortion.

spherically symmetrical potentials are assumed. For the region outside the ellipsoids, the rule of the paragraph above has to be extended. The spherically symmetrical inside potentials are not constant throughout the ellipsoidal surfaces, and therefore, for each atomic species, we make an average of the inside potential at the points where the ellipsoid touches neighboring ellipsoids. The constant outside is then defined as the average, among the atomic species, of the averages above.

To make these definitions clearer, we show how to calculate the potential part $V_{ij}(\mathbf{r})$ of the strain Hamil-

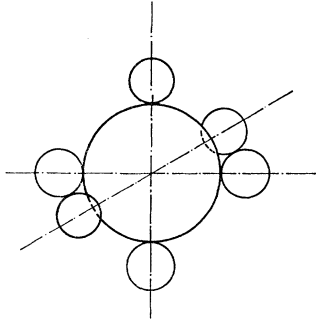


FIG. 2. Atom of Pb surrounded by six Te.

tonian of Eq. (2). Consider a uniaxial strain along an arbitrary direction. Orient the z axis along the direction of strain, therefore making the strain tensor have the form $\epsilon_{ij} = \delta_{3,i}\delta_{j,3}$. Let $v_{Pb}(r)$ and $v_{Te}(r)$ be the spherically symmetrical potentials inside the lead and tellurium ellipsoids. Inside a lead sphere, the potential, in the normal lattice, is $V_0(\mathbf{r}) = v_{Pb}(x, y, z)$, and the potential in the strained lattice is $V^S(\mathbf{r}) = v_{Pb}(x, y, z)$. There-

TABLE IX. Matrix elements of the isotropic strain Hamiltonian^a for the Γ_{15}^{C-} state (eV).

Representation	Partner	Γ_{15}^{C-}		
		x	y	z
Γ_{15}^{C-}	x	-3.975	0	0
	y	0	-3.975	0
	z	0	0	-3.975

^a The isotropic strain tensor is here defined as the tensor δ_{ij} .

fore, the contribution $\epsilon_{ij}V_{ij}(\mathbf{r})$ to the strain Hamiltonian is

$$\epsilon V_{zz}(\mathbf{r}) = \epsilon \left[\frac{v_{Pb}(x, y, z + \epsilon z) - v_{Pb}(x, y, z)}{\epsilon} \right]_{\epsilon=0} = \epsilon v_{Pb}'(r) z^2 / r. \quad (6)$$

Similarly, inside a tellurium sphere we get the contribution

$$\epsilon V_{zz}(\mathbf{r}) = \epsilon v_{Te}'(r) z^2 / r. \quad (7)$$

For the contribution outside the spheres, we first consider a lead atom. (See Fig. 2.) This sphere touches six

TABLE X. Matrix elements of the uniaxial strain Hamiltonian^a along (001) for the state Γ_{15}^{C-} (eV).

Representation	Partner ^b	Γ_{15}^{C-}			
		Reduced representation	x	y	z
Γ_{15}^{C-}	x	Γ_5^{T-}	-2.633	0	0
	y	Γ_5^{T-}	0	-2.633	0
	z	Γ_2^{T-}	0	0	1.291

^a The uniaxial strain along (001) is here defined as the tensor v_{ij} if $\mathbf{v} = (001)$.

^b The coordinates x , y , and z are along the directions (100), (010), and (001), respectively.

TABLE XI. Matrix elements of the uniaxial strain Hamiltonian along (111) for the Γ_{15}^{C-} state (eV).^a

Representation	Partner ^b	Reduced representation	Γ_{15}^{C-}		
			x	y	z
Γ_{15}^{C-}	x	Γ_3^{R-}	1.309	0	0
	y	Γ_3^{R-}	0	1.309	0
	z	Γ_2^{R-}	0	0	-6.593

^a The uniaxial strain tensor along (111) is here defined as the tensor v_{ij} if $\mathbf{v} = (111)/\sqrt{3}$.

^b The coordinates x , y , z are along the directions $(1\bar{1}0)$, $(11\bar{2})$, and (111) , respectively.

neighboring tellurium spheres, and the points of tangency, in the normal lattice, are $(R_{Pb}, 0, 0)$, $(0, R_{Pb}, 0)$, $(0, 0, R_{Pb})$, $(-R_{Pb}, 0, 0)$, $(0, -R_{Pb}, 0)$, and $(0, 0, -R_{Pb})$. Here R_{Pb} stands for the radius of the lead spheres. If we denote by \mathbf{r}_i any one of these six vectors, and by \mathbf{u} a

TABLE XII. Matrix elements of the isotropic strain Hamiltonian^a for point L along (111) (eV).

Representation	Partner ^b	L					
		x	y	z	1	zx	zy
L_3^{C-}	x	-5.29	0	0	0	0	0
	y	0	-5.29	0	0	0	0
L_2^{C-}	z	0	0	-4.78	0	0	0
L_1^{C+}	1	0	0	0	-16.33	0	0
L_3^{C+}	zx	0	0	0	0	-4.98	0
	zy	0	0	0	0	0	-4.98

^a The isotropic strain tensor is here defined as the tensor δ_{ij} .

^b The coordinates x , y , and z are along the directions $(1\bar{1}0)$, $(11\bar{2})$, and (111) , respectively.

unit vector along the strain direction, the distance from the i th point of tangency to the center of the lead ellipsoid, in the deformed lattice, becomes

$$d_i = [(\mathbf{r}_i \times \mathbf{u})^2 + (\mathbf{r}_i \cdot \mathbf{u})^2 (1 + \epsilon)^2]^{1/2} = R_{Pb} + \epsilon (\mathbf{r}_i \cdot \mathbf{u}) / R_{Pb},$$

so that the inside potential at the i th point of tangency

TABLE XIII. Matrix elements of the uniaxial strain Hamiltonian along (111)^a for point L along (111) (eV).

Representation	Partner ^b	L					
		x	y	z	1	zx	zy
L_3^{C-}	x	3.49	0	0	0	0	0
	y	0	3.49	0	0	0	0
L_2^{C-}	z	0	0	3.93	0	0	0
L_1^{C+}	1	0	0	0	1.53	0	0
L_3^{C+}	zx	0	0	0	0	1.79	0
	zy	0	0	0	0	0	1.79

^a The uniaxial strain tensor along (111) is here defined as the tensor v_{ij} if $\mathbf{v} = (111)/\sqrt{3}$.

^b The coordinates x , y , and z are along the directions $(1\bar{1}0)$, $(11\bar{2})$, and (111) , respectively.

TABLE XIV. Matrix elements of the uniaxial strain Hamiltonian along (001)^a for point *L* along (111) (eV).

Representation	Partner ^b	Reduced representation	L_3^{C-}		L_2^{C-}	L_1^{C+}	L_3^{C+}	
			<i>x</i>	<i>y</i>	<i>z</i>	1	<i>zx</i>	<i>zy</i>
			L_1^{T-}	L_2^{T-}	L_2^{T-}	L_1^{T+}	L_2^{T+}	L_1^{T+}
L_3^{C-}	<i>x</i>	L_1^{T-}	2.02	0	0	0	0	0
	<i>y</i>	L_2^{T-}	0	-5.55	5.96	0	0	0
L_2^{C-}	<i>z</i>	L_2^{T-}	0	5.96	-1.60	0	0	0
L_1^{C+}	1	L_1^{T+}	0	0	0	-5.44	0	7.19
L_3^{C+}	<i>zx</i>	L_2^{T+}	0	0	0	0	1.13	0
	<i>zy</i>	L_1^{T+}	0	0	0	7.19	0	-4.45

^a The uniaxial strain tensor along (001) is here defined as the tensor $v_i v_j$ if $\mathbf{v} = (001)$.

^b The coordinates *x*, *y*, and *z* are along the directions (110), (112), and (111), respectively.

becomes

$$v_{\text{Pb}}(d_i) = v_{\text{Pb}}(R_{\text{Pb}}) + v_{\text{Pb}}'(R_{\text{Pb}})\epsilon(\mathbf{r}_i \cdot \mathbf{u})^2 / R_{\text{Pb}}.$$

Making an average over the six points of tangency, we get

$$(\text{average for Pb}) = v_{\text{Pb}}(R_{\text{Pb}}) + \epsilon v_{\text{Pb}}'(R_{\text{Pb}})R_{\text{Pb}}/3.$$

Finally, the constant value outside the ellipsoids is assumed to be the average between the averages above, for lead and for tellurium:

$$(\text{constant potential}) = [v_{\text{Pb}}(R_{\text{Pb}}) + v_{\text{Te}}(R_{\text{Te}})]/2 + \epsilon [v_{\text{Pb}}'(R_{\text{Pb}})R_{\text{Pb}} + v_{\text{Te}}'(R_{\text{Te}})R_{\text{Te}}]/6,$$

from which it follows that the potential part of the strain Hamiltonian outside the spheres is given by

$$\epsilon V_{zz}(\mathbf{r}) = \epsilon [v_{\text{Pb}}'(R_{\text{Pb}})R_{\text{Pb}} + v_{\text{Te}}'(R_{\text{Te}})R_{\text{Te}}]/6. \quad (8)$$

Equations (6) and (8), together with Eq. (2), define the strain Hamiltonian completely. The reader may observe that the model we used, to derive the contribution $V_{ij}(\mathbf{r})$, is neither the rigid ion nor the deformable ion model,⁸ but one that comes directly

from the APW method. Inside the spheres, our model resembles the rigid-ion model.

Once the uniaxial strain Hamiltonian is known, we have to calculate its matrix element between two general symmetrized combinations of augmented plane waves.⁹ This is a very long calculation and cannot be reproduced here. It is believed that the interested reader could easily remake it, if he is familiar with the formalism of the APW method.^{9,10} The final expressions for the matrix element of the strain Hamiltonian were carefully checked. In particular, the "empty lattice test" was made, and the deformation potentials for isotropic expansion were compared against a recalculation of the band for a larger lattice parameter.

The numerical results are presented in Tables IX–XV. In each table, the values of the matrix elements for unit strains are given. A unit isotropic strain is here defined as the strain δ_{ij} , while a unit uniaxial strain along $(v_1 v_2 v_3)$ is defined as $v_i v_j$. Whenever the unit strain reduces the group of the wave vector, the names of the representations of the reduced group are given. The notation follows that of Tables III–VIII. It is important to observe that the nonzero entries are

 TABLE XV. Matrix elements of the uniaxial strain Hamiltonian along (111)^a for point *L* along (111) (eV).

Representation	Partner ^b	Reduced representation	L_3^{C-}		L_2^{C-}	L_1^{C+}	L_3^{C+}	
			<i>x</i>	<i>y</i>	<i>z</i>	1	<i>zx</i>	<i>zy</i>
			L_1^{R-}	L_2^{R-}	L_2^{R-}	L_1^{R+}	L_2^{R+}	L_1^{R+}
L_3^{C-}	<i>x</i>	L_1^{R-}	-1.05	0	0	0	0	0
	<i>y</i>	L_2^{R-}	0	-5.98	4.44	0	0	0
L_2^{C-}	<i>z</i>	L_2^{R-}	0	4.44	-3.44	0	0	0
L_1^{C+}	1	L_1^{R+}	0	0	0	-7.77	0	4.35
L_3^{C+}	<i>zx</i>	L_2^{R+}	0	0	0	0	-1.66	0
	<i>zy</i>	L_1^{R+}	0	0	0	4.35	0	-3.96

^a The uniaxial strain tensor along (111) is here defined as the tensor $v_i v_j$ if $\mathbf{v} = (111)/\sqrt{3}$.

^b The coordinates *x*, *y*, and *z* are along the directions (110), (112), and (111), respectively.

⁸ J. M. Ziman, *Electrons and Phonons* (Oxford University Press, London, 1960), 1st ed., Chap. 5, p. 183.

⁹ J. H. Wood, *Phys. Rev.* **126**, 517 (1962).

¹⁰ J. C. Slater, *Phys. Rev.* **51**, 846 (1937).

not all independent, because there is a general relation among them, that we now consider. Let (K) denote the group of the wave vector \mathbf{k} . Let (K) have K elements and let (A) be the complex of operations such that

$$(K) \times (A) = \text{point group of the crystal.}$$

Consider a representation μ of (K) and suppose that, because of a uniaxial strain along \mathbf{v} , the representation breaks into representations μ_1, \dots, μ_v of the subgroup of (K) that leaves the strain invariant:

$$\mu = \mu_1 + \dots + \mu_v.$$

Let μ have dimension n_μ and $\mu_i (i=1, \dots, v)$ have dimension n_{μ_i} . Similarly, because of a uniaxial strain

along $A\mathbf{v}$, obtained from \mathbf{v} by an operation of the complex (A) , the representation μ breaks into representations μ_1, \dots, μ_{Av} . Denoting by $(\mu_i | A\mathbf{v} | \mu_i)$ the matrix element of the unit uniaxial strain Hamiltonian along $A\mathbf{v}$, for the representation μ_i coming out of the reduction of the representation μ , and by $(\mu | \text{iso} | \mu)$ the matrix element of the unit isotropic strain Hamiltonian for representation μ , the general linear relation between matrix elements is

$$K \sum_{(A)} \left[\sum_{i=1}^{Av} n_{\mu_i} (\mu_i | A\mathbf{v} | \mu_i) \right] = 16n_\mu (\mu | \text{iso} | \mu). \quad (5)$$

Equation (5) implies the following relations among the entries of Tables IX–XV:

$$\begin{aligned} (\Gamma_2^{T-} | 001 | \Gamma_2^{T-}) + 2(\Gamma_3^{T-} | 001 | \Gamma_3^{T-}) &= (\Gamma_{15}^{C-} | \text{iso} | \Gamma_{15}^{C-}), \\ (\Gamma_2^{R-} | 111 | \Gamma_2^{R-}) + 2(\Gamma_3^{R-} | 111 | \Gamma_3^{R-}) &= (\Gamma_{15}^{C-} | \text{iso} | \Gamma_{15}^{C-}), \\ 3(L_1^{R+} | 11\bar{1} | L_1^{R+}) + (L_1^{C+} | 111 | L_1^{C+}) &= \frac{4}{3}(L_1^{C+} | \text{iso} | L_1^{C+}), \\ 3(L_2^{R-} | 11\bar{1} | L_2^{R-}) + (L_2^{C-} | 111 | L_2^{C-}) &= \frac{4}{3}(L_2^{C-} | \text{iso} | L_2^{C-}), \\ 3(L_1^{R+} | 11\bar{1} | L_1^{R+}) + 3(L_2^{R+} | 11\bar{1} | L_2^{R+}) + 2(L_3^{C+} | 111 | L_3^{C+}) &= \frac{8}{3}(L_3^{C+} | \text{iso} | L_3^{C+}), \\ 3(L_1^{R-} | 11\bar{1} | L_1^{R-}) + 3(L_2^{R-} | 11\bar{1} | L_2^{R-}) + 2(L_3^{C-} | 111 | L_3^{C-}) &= \frac{8}{3}(L_3^{C-} | \text{iso} | L_3^{C-}), \\ (L_1^{T+} | 001 | L_1^{T+}) &= \frac{1}{3}(L_1^{C+} | \text{iso} | L_1^{C+}), \\ (L_2^{T-} | 001 | L_2^{T-}) &= \frac{1}{3}(L_2^{C-} | \text{iso} | L_2^{C-}), \\ (L_1^{T+} | 001 | L_1^{T+}) + (L_2^{T+} | 001 | L_2^{T+}) &= \frac{2}{3}(L_3^{C+} | \text{iso} | L_3^{C+}), \\ (L_1^{T-} | 001 | L_1^{T-}) + (L_2^{T-} | 001 | L_2^{T-}) &= \frac{2}{3}(L_3^{C-} | \text{iso} | L_3^{C-}). \end{aligned}$$

IV. DISCUSSION

When we consider the spin-orbit interaction, the band picture becomes that of Fig. 3.¹ Again, this is a schematic drawing. The actual band calculation gave an $L_6^-(L_2^-)$ state slightly below the $L_6^+(L_1^+)$. This order of levels would make a metal instead of a semiconductor. It is felt here that a lack of self-consistency in the potential can cause small displacements in the position of the levels. The two L_6^- states, namely, the one coming from L_3^- and the one coming from L_2^- , mix. The same thing happens to the two L_6^+ states.

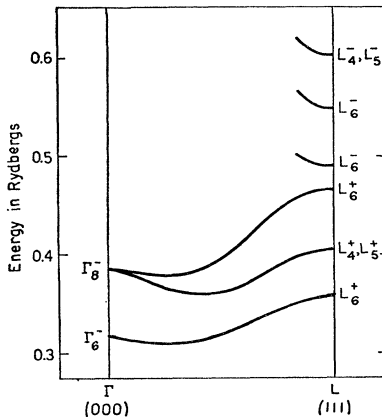


FIG. 3 Some important double-group states in PbTe (schematic).

Unfortunately, the amount of this mixing cannot be determined accurately, because the potential is not self-consistent. But we shall assume that it is not large.

The most important consequence of the spin-orbit interaction, for point L , is the removal of degeneracies.³ Because the levels are nondegenerate, the effects of strain in any of the states at L , in the first order, can be described by

$$\delta E = D_{ij} \epsilon_{ij}, \quad (9)$$

where δE is the change in the energy of the state, and D_{ij} is the deformation potential tensor. No simple equation like Eq. (9) exists for degenerate levels. It can be shown that the deformation potential tensor for the nondegenerate states at L can be written as

$$D_{ij} = D_a \delta_{ij} + D_u u_i u_j,$$

where $\mathbf{u} = (u_1 u_2 u_3)$ is the unit vector along the (111) direction. Therefore, the parameters D_a and D_u , for any given state with wave function ψ , can be calculated by the following relations:

$$(\psi | \text{iso} | \psi) = D_{\text{iso}} = 3D_a + D_u,$$

$$(\psi | 111 | \psi) = D_a + D_u.$$

The values of D_{iso} , D_a , and D_u , for the important states at L , are given in Table XVI. Because of the spin-orbit mixing of the L_6 states, the final D_a and D_u

will have the form

$$D_{u,d}(L_6^+) = (1-p)D_{u,d}[L_6^+(L_1^+)] + pD_{u,d}[L_6^+(L_3^+)],$$

$$D_{u,d}(L_6^-) = (1-q)D_{u,d}[L_6^-(L_2^-)] + qD_{u,d}[L_6^-(L_3^-)].$$

We assume that the spin-orbit mixing is small, so that q and p are small for the lowest L_6^- and the highest L_6^+ , and large for the highest L_6^- and lowest L_6^+ . It is important to note that, in the first order, the isotropic strain and the uniaxial strain along (111) are sufficient to determine the behavior for all states at L . In the second and higher orders, though, the uniaxial strains along (001) and (11 $\bar{1}$) are also important.

The spin-orbit interaction splits the Γ_{15}^- state, at the zone center, into Γ_8^- and Γ_6^- . Γ_8^- becomes higher than Γ_6^- by 0.943 eV. Since there have been reports suggesting an important valence band maximum at the center of the zone,⁷ and according to the band structure calculation this can only be a Γ_8^- state, it is important to consider the deformation potential of this state in detail.

Γ_8^- is a fourfold degenerate state and therefore the problem of the effects of a strain on this state are found, once the 4×4 matrix of the strain Hamiltonian corresponding to Γ_8^- is known. Proceeding from an argument similar to that of Luttinger,¹¹ Kleiner and Roth⁴ suggested the following form for this 4×4 matrix:

$$H = H_0 + D_d(\epsilon_{xx} + \epsilon_{yy} + \epsilon_{zz})$$

$$+ \frac{2}{3}D_u[(J_x^2 - J^2/3)\epsilon_{xx} + \text{c.p.}]$$

$$+ \frac{2}{3}D_{u'}[(J_y J_z + J_z J_y)\epsilon_{yz} + \text{c.p.}],$$

where H_0 is the 4×4 diagonal matrix of the unperturbed Hamiltonian, the D 's are the deformation potentials, and c.p. means a cyclic permutation. J_x, J_y, J_z are three 4×4 matrices that satisfy the commutation relations of an angular momentum, with

$$J^2 = J_x^2 + J_y^2 + J_z^2 = \frac{3}{2}$$

and such that in a transformation of the basis that corresponds to a rotation of the point group, J_x, J_y, J_z transform as the components of an angular momentum. The explicit expressions for the 4×4 matrices J_x, J_y, J_z are given by Luttinger.¹¹

Therefore, from the entries of Tables IX–XV we can find the values of $D_d, D_u,$ and $D_{u'}$ which are listed in Table XVII.

There have been published in the literature a number of experiments whose results are related to the behavior of the material under strain. The first set of experiments related to the deformation potentials of the material is the thermal expansion of the gap, determined by two observers^{12,13} to be about 4×10^{-4} eV/°C. From this number we can get a rough estimate of $D_{\text{iso}}(\text{conduction}) - D_{\text{iso}}(\text{valence})$ if we take into account that the coeffi-

 TABLE XVI. Deformation potentials for states at L (eV).

	D_{iso}	D_d	D_u	D_d/D_u
$L_{4,6}^-(L_3^-)$	-5.29	-4.39	7.89	-0.557
$L_6^-(L_2^-)$	-4.78	-4.36	8.29	-0.526
$L_6^+(L_1^+)$	-16.33	-8.93	10.46	-0.853
$L_{4,6}^+(L_3^+)$	-4.98	-3.38	5.18	-0.652

cient of thermal expansion for PbTe is $27 \times 10^{-6}/^\circ\text{C}$. Therefore $D_{\text{iso}}(\text{conduction}) - D_{\text{iso}}(\text{valence}) = 15$ eV. Inaccurate though this number may be, and despite the fact that the variation of the gap depends on many things besides the thermal expansion, this calculation points to the fact that the valence band is certainly $L_6^+(L_1^+)$ and not $L_4^+(L_3^+)$ as was thought at first, since the latter would not be consistent with a thermal expansion of the gap. Indeed, from Table XVI the reader can observe that

$$D_{\text{iso}}[L_6^-(L_2^-)] - D_{\text{iso}}[L_4^+(L_3^+)]$$

is very small and not compatible with an appreciable variation of the energy gap with either temperature or pressure. However, the value 11.6 eV for $D_{\text{iso}}[L_6^-(L_2^-)] - D_{\text{iso}}[L_6^+(L_1^+)]$, is consistent.

The variation of the energy gap with pressure has been measured optically,¹⁴ and the results point to a pressure coefficient between -7.5×10^{-6} and -9.0×10^{-6} eV cm²/kg. If we use the value of the elastic constant $c_{11} + 2c_{12} = 12.48 \times 10^{11}$ dyn/cm² as reported in the literature, and since a strain $-\epsilon_{ij}$ corresponds to a pressure

$$P = (c_{11} + 2c_{12})\epsilon,$$

we get

$$D_{\text{iso}}(\text{conduction}) - D_{\text{iso}}(\text{valence}) = 9.5\text{--}11.4 \text{ eV}.$$

This result is in excellent agreement with the theoretical calculation. The latter one is 11.6 eV, assuming no spin-orbit mixing between L_3^+ and L_1^+ , and 9.4 eV for the strongest *coupling* that would still preserve L_6^+ as the highest valence state.

The mobility of PbTe was extensively studied by Lyden¹⁵ among other authors.^{16,17} It seems very well established that for both bands, at room temperature, the main scattering mechanism is due to lattice vibrations, since only this mechanism can justify a relaxation

 TABLE XVII. Deformation potentials for Γ_8^- (eV).

D_d	D_u	$D_{u'}$
-1.33	-1.96	3.95

¹⁴ W. Paul (private communication).

¹⁵ H. A. Lyden, Electrical Engineering Department, MIT, Doctoral thesis, 1962 (unpublished).

¹⁶ E. Z. Gershtein, T. S. Stavitskaia, and L. S. Stil'bans, Zh. Techn. Fiz. **11**, 2472 (1957) [English transl.: Soviet-Phys.—Techn. Phys. **2**, 2302 (1957)].

¹⁷ R. S. Allgaier and W. W. Scanlon, Phys. Rev. **111**, 1029 (1958).

¹¹ J. M. Luttinger, Phys. Rev. **102**, 1030 (1959).

¹² A. F. Gibson, Proc. Phys. Soc. (London) **B65**, 378 (1952).

¹³ D. G. Avery, Proc. Phys. Soc. (London) **B66**, 133 (1953); **67** (1954).

TABLE XVIII. Comparison of results.

	D_{iso} (conduction) $-D_{\text{iso}}$ (valence)	D_u (conduction)	D_u (valence)
Calculated ^a	9.4–11.6 eV
Pressure experiment	9.5–11.4 eV
Thermal expansion ^b	15.0 eV
Calculated	...	8.3 eV	10.5 eV
Piezoresistance ^c	...	2.6 eV	4.0 eV
Mobility ^d	...	27.0 eV	60.0 eV

^a The exact value cannot be determined without precisely knowing the energy separation between L_1^+ and L_3^+ . The spin-orbit mixing of L_1^+ and L_3^+ lowers the coefficient from 11.6 eV to a minimum value of 9.4 eV. This lower limit is calculated from the minimum energy separation between L_1^+ and L_3^+ , compatible with the requirement of the highest valence state being $L_6^+(L_1^+)$.

^b Thermal variation of the energy gap was wholly attributed to the thermal expansion of the lattice.

^c Includes no correction for the variation of the mobilities with strain, and assumes nondegenerate statistics.

^d Assuming a one-acoustical-phonon intravalley scattering.

time proportional to $E^{-1/2}$. On the other hand, if we assume that the lattice scattering is of the one-phonon acoustical type, we expect a free carrier mobility proportional to $T^{-3/2}$, which does not compare well with the $T^{-5/2}$ law observed for both holes and electrons in PbTe. In his work on the free carrier mobility in PbTe, Lyden, in agreement with other authors,¹⁸ concludes that the deviation from the $T^{-3/2}$ law might very well come from the variation of the effective masses with temperature. According to Lyden, the conductivity effective mass might vary by as much as a factor of 2 between liquid helium and room temperature.

Herring and Vogt¹⁹ have studied the one-phonon scattering in an anisotropic valley and derived the following formula for the mobility:

$$\mu = \frac{2^{3/2} \pi^{1/2} \hbar^4 c_l (1/m_{11} + 2/m_1) f}{9(kT)^{3/2} D_u^2 (m_{11} m_1^2)^{1/2}},$$

where c_l is a combination of elastic constants and f is a function that depends on the ratio D_d/D_u , on the effective mass ratio m_{11}/m_1 and on the elastic constants. We have calculated f for different values of D_d/D_u , for the elastic constants reported in the literature, and for different effective mass ratios. For D_d/D_u in the range -3 to 3 , the function f changed only by 10% on varying m_{11}/m_1 from 2 to 8, which makes it possible to know f for a given D_d/D_u even though the effective mass ratio is not quite well known. From this calculation we concluded that for $-1 \leq D_d/D_u \leq 0$, $f \approx 1$, while for $D_d/D_u \leq -1$, $f \approx (D_d/D_u)^{-2}$. If we assume a ratio D_d/D_u between -1 and 0 , as our calculations suggest for the bands at L , we obtain from Lyden's results $|D_u(\text{conduction})| = 27$ eV and $|D_u(\text{valence})| = 60$ eV. Although the value of D_u for the conduction band is not impossible, the value for the valence band seems

¹⁸ I. Smirnov, B. Moizhes, and E. Nensberg, Fiz. Tverd. Tela 2, 1992 (1960) [English transl.: Soviet Phys.—Solid State 2, 1793 (1961)].

¹⁹ C. Herring and E. Vogt, Phys. Rev. 101, 944 (1956).

much too large to be acceptable (5 to 10 times larger than what has been obtained for other materials, to which PbTe should be comparable).¹⁹

The piezoresistance of extrinsic samples of PbTe has also been the object of some study, of which the work of Ilisavskii²⁰ seems the most extensive. Using the formula derived by Herring and Vogt¹⁹

$$m_{44} = \pm D_u(\mu_{11} - \mu_1)/9kT\mu, \quad (10)$$

which relates the elastoresistance coefficient m_{44} to the deformation potential D_u and the mobility ratio $(\mu_{11} - \mu_1)/\mu$, Ilisavskii estimated that

$$D_u(\text{conduction}) = 2.6 \text{ eV}, \quad D_u(\text{valence}) = 4 \text{ eV}$$

(see Ref. 21). Here we recall that the coefficients m_{11} , m_{12} , m_{44} are the coefficients that relate the 3×3 matrix $(\Delta\rho/\rho)_{ij}$ —which is a symmetric matrix according to Onsager's principle—to the strain, and therefore they are analogous to the elastic constants that also relate two symmetric tensor, namely stress and strain. The Herring-Vogt formula was derived assuming that only the relative motion of equivalent valleys contributed to the elastoresistance m_{44} . This is known to be an oversimplification, though one can improve on the estimation of D_u from Eq. (10) using only that part of m_{44} that is proportional to T^{-1} , as suggested by Pikus and Bir.²² The argument used by these authors is that the other factors contributing to the elastoresistance m_{44} , namely, the variation of the effective masses and of the relaxation time with strain, should be almost independent of temperature, a fact which the enormous thermal variation of the effective masses, as determined by Lyden,¹⁸ clearly refutes. Also, Eq. (10) is only valid for nondegenerate statistics. Ilisavskii's samples had 10^{18} carriers per cc and were somewhat degenerate. The use of Eq. (10) in these cases underestimates the deformation potential D_u .

For the reader's convenience we present a comparison of the results in Table XVIII. The estimates of

$$D_{\text{iso}}(\text{conduction}) - D_{\text{iso}}(\text{valence})$$

are in excellent agreement with experiment. On the other hand, aside from small deviations, the calculated band structure of lead telluride seems to be consistent with the experimental evidence. The $\mathbf{k} \cdot \mathbf{p}$ perturbation, for instance, and our knowledge of the effective masses are compatible.²³ All these facts give a measure of confidence in our results. The biggest problem in a band calculation is the crystal potential. Once the potential is properly defined, the APW method becomes a very

²⁰ Yu. V. Ilisavskii, Fiz. Tverd. Tela 4, 918 (1962) [English transl.: Soviet Phys.—Solid State 4, 674 (1962)].

²¹ We corrected Ilisavskii's values for D_u because of an apparent error in sign and because the author had no experimental results for c_{44} .

²² G. E. Pikus and G. L. Bir, Fiz. Tverd. Tela 4, 2090 (1962) [English transl.: Soviet Phys.—Solid State 4, 1530 (1963)].

²³ G. W. Pratt, Jr., and L. G. Ferreira, paper given at the International Conference on the Physics of Semiconductors, Paris, 1964 (unpublished).

precise and practical one for a calculation of the band or of a perturbation thereon. But a numerical estimate of the errors cannot precede a better experimental knowledge of the material.

There is something disturbing about Table XVIII. The values for the uniaxial strain potentials are in bad disagreement. In our opinion, the results from the mobility measurements only prove that the intravalley acoustical scattering is an improper model for PbTe: another kind of scattering must be thought of. The results from the piezoresistance experiment are not too reliable; at least, let us not rely on them more than Ilisavskii does.²⁰ It is not that Ilisavskii's measurements are doubtful, but that the model he assumed to derive the numbers for the deformation potentials is too simple for the complex situation in PbTe. In particular, Ilisavskii was not able, for lack of data, to compensate the degeneracy of the electronic gas. Depending on the degree of degeneracy, his model can underestimate D_u by a factor of 2, 3, or more, which would bring his numbers much closer to ours. So, it is very possible that our numbers are very near the truth.

Finally, a word about previous works. Kleinman and Goroff have calculated the deformation potentials for

silicon.²⁴ Their work differs from the present one in that:

(1) In the case of silicon, a uniaxial strain can remove the inversion center; and there is no such complication in PbTe.

(2) Their method was based on the orthogonalized-plane-wave method, and ours is based on the APW.

(3) There is the all-important problem of definition of the crystal potential. As long as the potential is not self-consistent, it is difficult to know, *a priori*, how good it is. The only possible basis to judge a potential lies in the quality of the results. It is the author's opinion that a good potential should consistently give good results, in terms of the order of levels, $\mathbf{k} \cdot \mathbf{p}$ perturbation, strain deformation or any other perturbation. And we are pleased with the results obtained so far.

ACKNOWLEDGMENT

The writer is specially indebted to Professor George W. Pratt, Jr. for suggesting this work and for his continued interest and support.

²⁴ I. Goroff and L. Kleinman, Phys. Rev. **132**, 1080 (1963).

Magnetoresistance of Iron Whiskers*

ACAR İŞİN AND R. V. COLEMAN

Department of Physics, University of Virginia, Charlottesville, Virginia

(Received 22 July 1964; revised manuscript received 23 October 1964)

Transverse magnetoresistance measurements on iron whiskers with axes along $\langle 100 \rangle$, $\langle 110 \rangle$, and $\langle 111 \rangle$ have been made in fields up to 50 kOe. Measurements have been made on whiskers with diameters ranging from 40 to 400 μ . Sharp minima observed in the rotation diagrams measured at 50 kOe for all three orientations are consistent with the existence of open orbits along $\langle 100 \rangle$ and $\langle 110 \rangle$ directions. The field dependence curves show a region of negative magnetoresistance at low fields and at high fields the resistance varies as B^m , where $1 < m < 2$. The extent of the negative magnetoresistance region depends both on the field orientation and the diameter of the whisker and appears to be correlated with the domain structure. A size effect has also been observed on the field dependence of resistance at high fields and on the residual resistance ratio $\rho_{RT}/\rho_{4.2^\circ}$. Values of $\rho_{RT}/\rho_{4.2^\circ}$ range from 200 to 2000 for the whiskers which have been measured.

INTRODUCTION

MAGNETORESISTANCE measurements on single crystals of ferromagnetic metals have recently been used to obtain preliminary information on the nature of the Fermi surface in these metals.^{1,2} In the case of iron, whiskers offer one of the best possibilities of obtaining well-oriented high-purity crystals for such studies. De Haas-van Alphen studies on iron whiskers

by Gold³ have already been very successful, and preliminary data on Hall effect and magnetoresistance have been reported by Dheer.⁴ Reed and Fawcett⁵ have also reported initial results on the magnetoresistance in iron whiskers along with data on strain annealed crystals.

In this paper we report on the results of transverse magnetoresistance measurements on iron whiskers grown by the hydrogen reduction of ferrous chloride.

* Research supported by the U. S. Atomic Energy Commission and the U. S. Office of Naval Research.

¹ E. Fawcett and W. A. Reed, Phys. Rev. Letters **9**, 336 (1962).

² E. Fawcett and W. A. Reed, Phys. Rev. **131**, 2463 (1963).

³ J. R. Anderson and A. V. Gold, Phys. Rev. Letters **10**, 227 (1963).

⁴ P. N. Dheer, Bull. Am. Phys. Soc. **9**, 550 (1964).

⁵ W. A. Reed and E. Fawcett, Phys. Rev. **136**, A422 (1964).